CrystEngComm

ROYAL SOCIETY OF CHEMISTRY

COMMUNICATION

View Article Online
View Journal | View Issue

Cite this: *CrystEngComm*, 2021, **23**, 2923

Received 4th February 2021,
Accepted 30th March 2021

DOI: 10.1039/d1ce00175b

rsc.li/crystengcomm

Two polymorphs of remdesivir: crystal structure, solubility, and pharmacokinetic study†

Kaxi Yu, Shuai Chen, Chander Amgoth, Guping Tang, Hongzhen Bai* and Xiurong Hu*

Two polymorphic phases of the antiviral drug remdesivir (RDV), namely RDV-I and RDV-II are prepared and structurally characterized by single-crystal X-ray diffraction. Both RDV-I and RDV-II are solvent-free but exhibit different packing patterns in their crystals. RDV-I and RDV-II feature different pharmacokinetics, as revealed by *in vitro* and *in vivo* studies. This work highlights the significance of remdesivir drug formulations on the pharmacokinetics and ultimately patient outcome when combating the coronavirus disease 2019 (Covid-19).

Remdesivir (RDV) is a broad-spectrum antiviral agent that obscures the viral RNA polymerase and evades proofreading of viral exonuclease, leading to the inhibition of virus replication.[1] Recent studies have demonstrated that RDV shows potent antiviral activity in combating coronavirus including the severe acute respiratory syndrome coronavirus (SARS-CoV).[2–7] RDV has also been arguably suggested as a therapeutic option for patients infected with corona virus disease 2019 (Covid-19).[4,8–14]

RDV is currently administered by injection, which poses some difficulties. In order to assess all possible forms of RDV administration, the pharmacokinetics of polymorphs of RDV are of interest and should be assessed. In combating Covid-19, the nature of drug formulations, such as co-crystals, salts, and polymorphisms should be considered as it has a significant impact on the stability, tableting and compression behaviors, solubility and dissolution profiles, and ultimately the pharmacokinetics of the product.[14,15] In this article, we showcase that two solvent-free polymorphic forms of RDV, namely, **RDV-I** and **RDV-II**, exhibit differences in physicochemical properties and pharmacokinetics. Polymorphism refers to the diversity of crystalline forms in which an active pharmaceutical ingredient (API) may exist. Specifically for RDV, it has been documented to exhibit four polymorphs (**RDV-I** to **RDV-IV**), but their accurate molecular connectivity remains elusive because of the lack of single-crystal diffraction data. Meanwhile, it was reported that **RDV-III** contained harmful CH_2Cl_2 solvent and **RDV-IV** was unstable in solution and quickly converted to **RDV-II**.[16,17] Therefore, two more stable crystal forms (**RDV-I** and **RDV-II**) with solvent-free were selected and investigated. To gain direct structural insights into these polymorphic behaviours of RDV, we have prepared RDV polymorphs **RDV-I** and **RDV-II** under various crystallization conditions and characterized their single crystal structures *via* X-ray crystallography.

RDV-I was obtained as colorless block single crystals (Fig. S1a, ESI†) from a mixed solvent of CH_2Cl_2 and MeOH at 5–10 °C, while **RDV-II** was obtained as trigonal prismatic single crystals (Fig. S1b, ESI†) from a MeCN solution by slowly decreasing the temperature of a saturated RDV solution from 90 °C to 25 °C. The powder X-ray diffraction (PXRD, Fig. 1) of both **RDV-I** and **RDV-II** are in good agreement with those reported,[17] and those simulated from the single-crystal data,

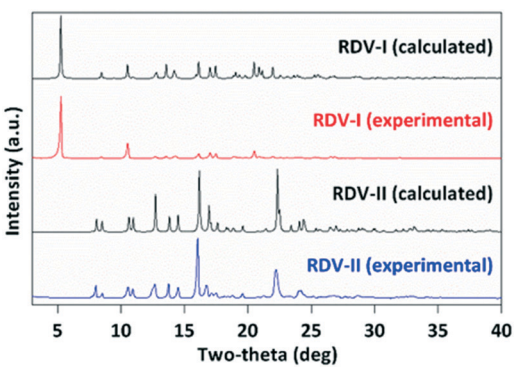

Fig. 1 Simulated and experimental PXRD patterns of RDV-I and RDV-II, showing a high consistency between the experimental and simulated diffraction patterns, and thus high bulk-phase purity of the prepared samples.

Department of Chemistry, Zhejiang University, Hangzhou 310028, Zhejiang, China. E-mail: hongzhen_bai@zju.edu.cn, huxiurong@zju.edu.cn

† Electronic supplementary information (ESI) available: Detailed experimental procedures, additional Tables and Figures. CCDC 2022369 and 2022370. For ESI and crystallographic data in CIF or other electronic format see DOI: 10.1039/d1ce00175b

indication of their high bulk phase purity. In FT-IR spectrum (Fig. S2, ESI†) and Raman spectrum (Fig. S3, ESI†) of RDV polymorphs there is different stretching frequencies for O–H and N–H groups, which is believed to be mainly caused by different hydrogen patterns of **RDV-I** and **RDV-II**. The result of differential scanning calorimetry (DSC) (Fig. S4 and S5, ESI†) reveals that **RDV-II** is a more thermodynamically stable polymorph.

Single crystal X-ray structure analysis indicated that **RDV-I** and **RDV-II** crystallize in the triclinic $P1$ and monoclinic $P2_1$ space groups, respectively (Table S1, ESI†). The asymmetric unit of **RDV-I** contains a pair of RDV molecules (Fig. 2a), whereas the asymmetric unit of **RDV-II** contains only one RDV molecule (Fig. 2b). A structure overlay (Fig. S6, ESI†) illustrates that the conformation of the two RDV molecules in **RDV-I** are similar but deviate significantly from that of **RDV-II**. This is due to the conformational flexibility enabled by the presence of single bonds that warrants sufficient rotational freedom, particularly those three single bonds around the phosphorus centers.

It is well-established that the variation of pharmaceutical polymorphic crystal forms may affect the solubility and dissolution rate of drug.[18–23] We thus investigated the solubility and dissolution properties of **RDV-I** and **RDV-II** in the aqueous system. As shown in Fig. 3a, the dissolution profiles of **RDV-I** are drastically different from those of **RDV-II** in water (pH 7). Specifically, **RDV-I** exhibits marginally faster dissolution rates and higher solubility than **RDV-II**. The solution of **RDV-I** reaches equilibrium after 50 min,

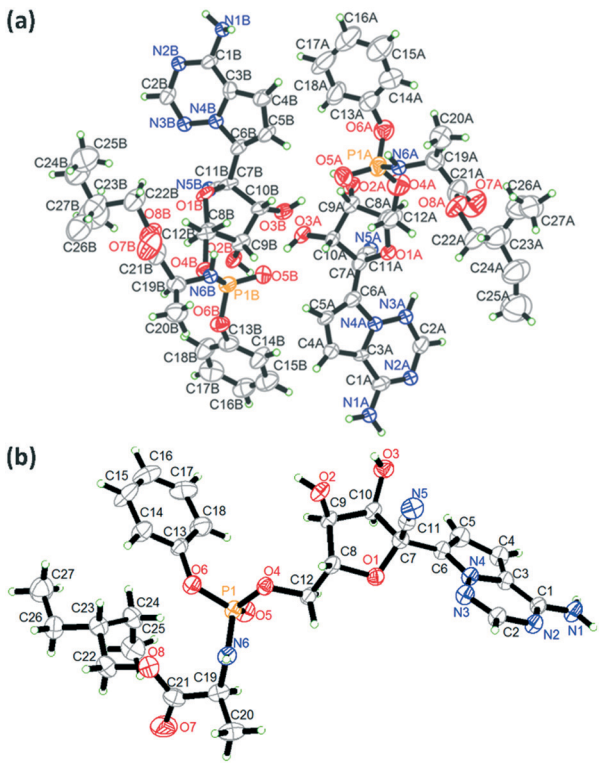

Fig. 2 The asymmetric units of **RDV-I** (a) and **RDV-II** (b).

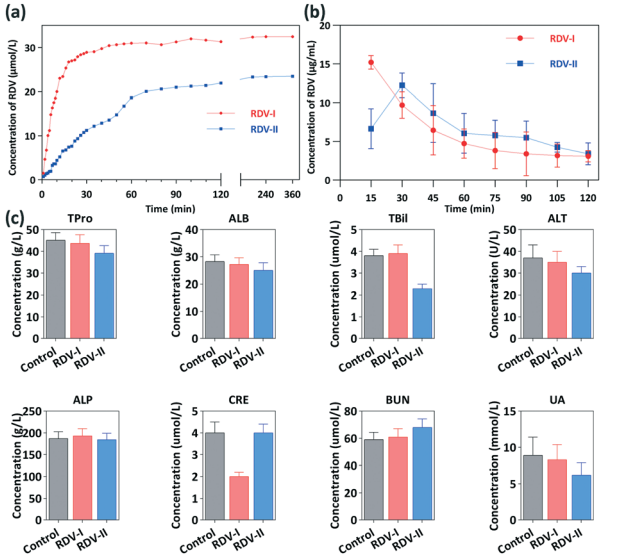

Fig. 3 Solution concentration-time profiles of **RDV-I** and **RDV-II** in water (a), *in vivo* pharmacokinetic profiles of **RDV-I** and **RDV-II** (b), blood indices of mice treated with PBS, **RDV-I**, **RDV-II** (c).

whereas 100 min is needed for **RDV-II**. Notably, after 24 h, the concentration of **RDV-I** is also approximately 20% higher than that of **RDV-II** (Fig. S7, ESI†).

For pharmacokinetic studies, ICR mice were randomly divided into two groups (8 for each group) and orally administered **RDV-I** and **RDV-II** with dosages of 8 mg kg^{-1}.[17] The blood was then collected from the orbital sinus with a heparinized syringe at 15, 30, 45, 60, 75, 90, 105, and 120 min after drug administration (Fig. 3b). High-performance liquid chromatography (HPLC) gives the area under the curve (AUC_{0-t}) values of 14.99 μg L^{-1} h for **RDV-I** and 12.72 μg L^{-1} h for **RDV-II**. Besides, **RDV-I** achieved the larger C_{max} value of 15.22 μg mL^{-1} at a shorter T_{max} of 15 min, while **RDV-II** attained the C_{max} value of 12.26 μg mL^{-1} at T_{max} of 30 min. **RDV-I** exhibits a 1.24-fold higher peak plasma concentration (C_{max}) and 1.18-fold higher AUC than **RDV-II** in mice. The concentrations of **RDV-I** and **RDV-II** were measured in 2 h, and the results suggest that RDV rapidly converted to the active nucleoside triphosphate form (GS-441524)[1,2,8] *in vivo* within 2 h. From these results, it is concluded that **RDV-I** manifested an enhanced concentration in the first 15 min and a faster conversion rate within 2 h, which coincided with the higher dissolution rate of **RDV-I**.

In order to assess the biosafety of **RDV-I** and **RDV-II**, the hepatic and kidney functions were then analyzed by determining the biochemical indices in blood (Fig. 3c).[24] Value of the hepatic function parameters (TPro, ALB, TBil, ALT, ALP) and the kidney function (CRE, BUN, UA) of the experimental groups was close to those of the control group, except that the TBil value of **RDV-I** and the CRE value of **RDV-II** were *ca.* half that of the control group. These results indicate that RDV treatments exert negligible impact on hepatic and kidney functions.

The dissolution rate, solubility, and the pharmacokinetic indices of **RDV-I** and **RDV-II** in mice, are largely depend on

the intermolecular associations between RDV molecules. It is thus important to address the pharmacokinetic difference between **RDV-I** and **RDV-II** based on their associations at the molecular level. Both **RDV-I** and **RDV-II** exhibit a two-dimensional (2D) hydrogen-bonded networks due to the presence of rich classical hydrogen-bonding donors (two –OH and one $–NH_2$ groups) and acceptors (such as –OH, –C≡N, and –P═O) in the RDV molecule. As shown in Fig. 4a, **RDV-I** associates with the adjacent equivalents to give a double-stranded chain structure along the crystallographic *a*-axis and featuring a $R_3^3(15)$ tape. Comparatively, O–H···O and N–H···O hydrogen-bonding interactions in **RDV-II** support a different type of double-stranded chain structure along the crystallographic *b*-axis featuring a $R_3^3(26)$ ring (Fig. 4b). It is interesting to note that the double-stranded chains of **RDV-I** are separated by the hydrophobic CH-based 2-ethylbutyl chain while the double-stranded chains of **RDV-II** are further associated with hydrogen-bonding interactions. These strikingly different supramolecular characteristics of **RDV-I** and **RDV-II** may serve to in part explain the observed differences in their dissolution rates and the pharmaceutics *in vivo*.

To assess and compare the intermolecular interactions and packing modes in **RDV-I** and **RDV-II**, Hirshfeld surfaces and two-dimensional (2D) fingerprint maps were generated using the program Crystal Explorer.[25–28] The deep-red spots on the Hirshfeld surface reveal the shortest N–H···O and O–H···O interactions where are the hydrogen bondings (Fig. 5). The blue spots on the surfaces correspond to C···H and H···H contacts. The 2D fingerprint plots (Fig. S8, ESI†) provide a more informative use of these quantities and reveals the comparison between RDV-I and RDV-II in a straightforward. It reveals that **RDV-II** features a greater

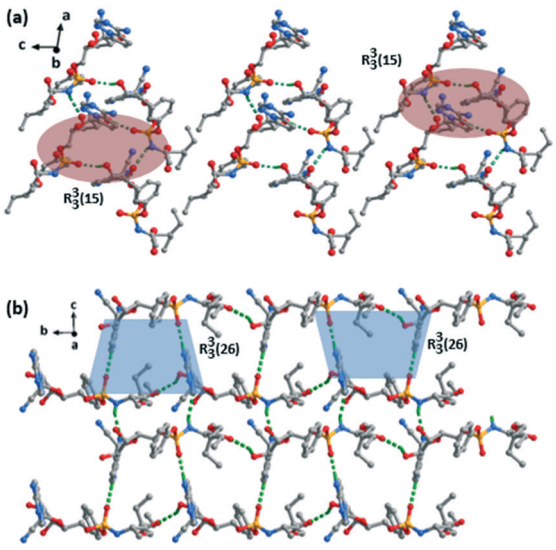

Fig. 4 The hydrogen-bonding network of **RDV-I** (a) and **RDV-II** (b). Hydrogen bonds are shown as green lines and H atoms not involved in the hydrogen-bonding have been omitted for clarity; color codes: P (orange), O (red), N (blue), C (gray), H (green).

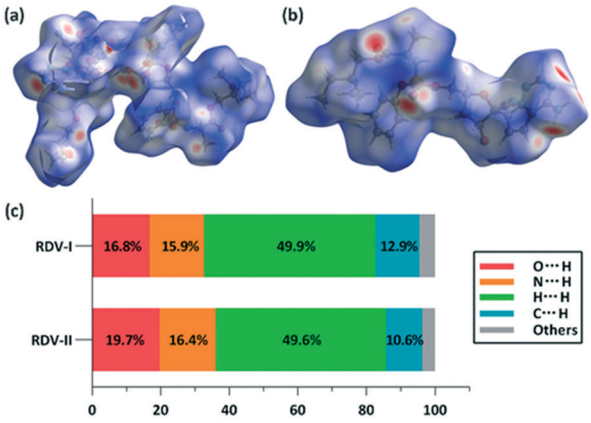

Fig. 5 Hirshfeld surfaces mapped with d_{norm} of **RDV-I** (a) and **RDV-II** (b), and the average relative contribution to the Hirshfeld surface for the various intermolecular contacts for **RDV-I** and **RDV-II** (c).

contribution from the hydrogen contacts (O···H, 19.7%; N···H 16.4%) than those of **RDV-I** (16.8%, 15.9%). In contrast, **RDV-I** contains a higher C···H hydrogen contacts' contribution (12.9%) than that of **RDV-II** (10.6%), corroborating that these observed in their crystal packing diagrams (Fig. 4). The analysis consistence with the higher contribution from stronger hydrogen bonding contacts and weaker short contacts of **RDV-II**.

To gain more insight into the intermolecular interactions, we conducted energy frameworks to assess the intermolecular interactions and packing modes of **RDV-I** and **RDV-II**. In the energy framework of **RDV-I**, cylindrical energy framework propagates along the *c*-direction comprising molecules linked by weak interactions (Fig. S9a, ESI†). On the contrary, multiple zigzag-shaped energy frameworks of **RDV-II** cross-linked to give an overall 2D grid (Fig. S9b, ESI†). Therefore, RDV molecules in **RDV-II** have better stability and dissociate more slowly in solvents when compared with that of **RDV-I**. Thus **RDV-I** has a faster dissolution rate and higher AUCs.

In summary, we characterized the single-crystal structures of **RDV-I** and **RDV-II** as two solvent-free polymorphs of RDV and disclosed that the solubility, pharmacokinetics, and biosafety might be linked to their different structural patterns of these two polymorphs. This work points to the potential of different polymorphs of RDV on the clinical application.

Author contributions

X. H., H. B. and G. T. conceived and supervised the projects and designed the research; K. Y. performed all experiments and data analysis, K. Y., H. B., and X. H. wrote the manuscript; S. C. helped to perform the experiments to get the materials; C. A. contributed through the technical assistance.

Conflicts of interest

There are no conflicts of interest to declare.

Acknowledgements

We thank Dr. Wen-Hua Zhang from Soochow University for his technical assistance for the article. We thank Mr. Guanneng Yu, Dr. Chun'guang Dai and Mr. Zhiguo Zheng from Zhejiang Ausun Pharmaceutical Co. Ltd. to provide the chemical materials. This work was supported by the National Natural Science Foundation of China (No. 51873185). The *in vivo* experiments were performed in accordance with the CAPN (China Animal Protection Law), which were approved by the Zhejiang University Institutional Animal Care and Use Committee in China (approval ID: ZJU20190018).

Notes and references

1 T. K. Warren, R. Jordan, M. K. Lo, A. S. Ray, R. L. Mackman, V. Soloveva, D. Siegel, M. Perron, R. Bannister, H. C. Hui, N. Larson, R. Strickley, J. Wells, K. S. Stuthman, S. A. Van Tongeren, N. L. Garza, G. Donnelly, A. C. Shurtleff, C. J. Retterer, D. Gharaibeh, R. Zamani, T. Kenny, B. P. Eaton, E. Grimes, L. S. Welch, L. Gomba, C. L. Wilhelmsen, D. K. Nichols, J. E. Nuss, E. R. Nagle, J. R. Kugelman, G. Palacios, E. Doerffler, S. Neville, E. Carra, M. O. Clarke, L. Zhang, W. Lew, B. Ross, Q. Wang, K. Chun, L. Wolfe, D. Babusis, Y. Park, K. M. Stray, I. Trancheva, J. Y. Feng, O. Barauskas, Y. Xu, P. Wong, M. R. Braun, M. Flint, L. K. McMullan, S. S. Chen, R. Fearns, S. Swaminathan, D. L. Mayers, C. F. Spiropoulou, W. A. Lee, S. T. Nichol, T. Cihlar and S. Bavari, *Nature*, 2016, **531**, 381–385.

2 M. L. Agostini, E. L. Andres, A. C. Sims, R. L. Graham, T. P. Sheahan, X. Lu, E. C. Smith, J. B. Case, J. Y. Feng, R. Jordan, A. S. Ray, T. Cihlar, D. Siegel, R. L. Mackman, M. O. Clarke, R. S. Baric and M. R. Denison, *MBio*, 2018, **9**(2), e00221-18.

3 S. De Meyer, D. Bojkova, J. Cinatl, E. Van Damme, C. Buyck, M. Van Loock, B. Woodfall and S. Ciesek, *Int. J. Infect. Dis.*, 2020, **97**, 7–10.

4 C.-C. Lai, T.-P. Shih, W.-C. Ko, H.-J. Tang and P.-R. Hsueh, *Int. J. Antimicrob. Agents*, 2020, **55**, 105924.

5 T. P. Sheahan, A. C. Sims, R. L. Graham, V. D. Menachery, L. E. Gralinski, J. B. Case, S. R. Leist, K. Pyrc, J. Y. Feng, I. Trantcheva, R. Bannister, Y. Park, D. Babusis, M. O. Clarke, R. L. Mackman, J. E. Spahn, C. A. Palmiotti, D. Siegel, A. S. Ray, T. Cihlar, R. Jordan, M. R. Denison and R. S. Baric, *Sci. Transl. Med.*, 2017, **9**, eaal3653.

6 C. Wu, Y. Liu, Y. Yang, P. Zhang, W. Zhong, Y. Wang, Q. Wang, Y. Xu, M. Li, X. Li, M. Zheng, L. Chen and H. Li, *Acta Pharm. Sin. B*, 2020, **10**, 766–788.

7 W. C. Yin, C. Y. Mao, X. D. Luan, D. D. Shen, Q. Y. Shen, H. X. Su, X. X. Wang, F. L. Zhou, W. F. Zhao, M. Q. Gao, S. H. Chang, Y. C. Xie, G. H. Tian, H. W. Jiang, S. C. Tao, J. S. Shen, Y. Jiang, H. L. Jiang, Y. C. Xu, S. Y. Zhang, Y. Zhang and H. E. Xu, *Science*, 2020, **368**, 1499–1504.

8 L. Dong, S. Hu and J. Gao, *Drug Discoveries Ther.*, 2020, **14**, 58–60.

9 J. Grein, N. Ohmagari, D. Shin, G. Diaz, E. Asperges, A. Castagna, T. Feldt, G. Green, M. L. Green, F. X. Lescure, E. Nicastri, R. Oda, K. Yo, E. Quiros-Roldan, A. Studemeister, J. Redinski, S. Ahmed, J. Bernett, D. Chelliah, D. Chen, S. Chihara, S. H. Cohen, J. Cunningham, A. D. Monforte, S. Ismail, H. Kato, G. Lapadula, E. L'Her, T. Maeno, S. Majumder, M. Massari, M. Mora-Rillo, Y. Mutoh, D. Nguyen, E. Verweij, A. Zoufaly, A. O. Osinusi, A. DeZure, Y. Zhao, L. Zhong, A. Chokkalingam, E. Elboudwarej, L. Telep, L. Timbs, I. Henne, S. Sellers, H. Cao, S. K. Tan, L. Winterbourne, P. Desai, R. Mera, A. Gaggar, R. P. Myers, D. M. Brainard, R. Childs and T. Flanigan, *N. Engl. J. Med.*, 2020, **382**, 2327–2336.

10 G. Li and E. De Clercq, *Nat. Rev. Drug Discovery*, 2020, **19**, 149–150.

11 V. R. Naik, M. Munikumar, U. Ramakrishna, M. Srujana, G. Goudar, P. Naresh, B. N. Kumar and R. Hemalatha, *J. Biomol. Struct. Dyn.*, 2020, 1–14.

12 J. M. Sanders, M. L. Monogue, T. Z. Jodlowski and J. B. Cutrell, *JAMA, J. Am. Med. Assoc.*, 2020, **323**, 1824–1836.

13 Y. Wang, D. Zhang, G. Du, R. Du, J. Zhao, Y. Jin, S. Fu, L. Gao, Z. Cheng, Q. Lu, Y. Hu, G. Luo, K. Wang, Y. Lu, H. Li, S. Wang, S. Ruan, C. Yang, C. Mei, Y. Wang, D. Ding, F. Wu, X. Tang, X. Ye, Y. Ye, B. Liu, J. Yang, W. Yin, A. Wang, G. Fan, F. Zhou, Z. Liu, X. Gu, J. Xu, L. Shang, Y. Zhang, L. Cao, T. Guo, Y. Wan, H. Qin, Y. Jiang, T. Jaki, F. G. Hayden, P. W. Horby, B. Cao and C. Wang, *Lancet*, 2020, **395**, 1569–1578.

14 M. Wang, R. Cao, L. Zhang, X. Yang, J. Liu, M. Xu, Z. Shi, Z. Hu, W. Zhong and G. Xiao, *Cell Res.*, 2020, **30**, 269–271.

15 L. F. Huang and W. Q. Tong, *Adv. Drug Delivery Rev.*, 2004, **56**, 321–334.

16 D. Siegel, H. C. Hui, E. Doerffler, M. O. Clarke, K. Chun, L. Zhang, S. Neville, E. Carra, W. Lew, B. Ross, Q. Wang, L. Wolfe, R. Jordan, V. Soloveva, J. Knox, J. Perry, M. Perron, K. M. Stray, O. Barauskas, J. Y. Feng, Y. Xu, G. Lee, A. L. Rheingold, A. S. Ray, R. Bannister, R. Strickley, S. Swaminathan, W. A. Lee, S. Bavari, T. Cihlar, M. K. Lo, T. K. Warren and R. L. Mackman, *J. Med. Chem.*, 2017, **60**, 1648–1661.

17 K. Brak, E. A. Carra, L. V. Heumann and N. Larson, *US Pat.*, WO/2018/204198, 2018.

18 N. Blagden, M. de Matas, P. T. Gavan and P. York, *Adv. Drug Delivery Rev.*, 2007, **59**, 617–630.

19 S. L. Morissette, O. Almarsson, M. L. Peterson, J. F. Remenar, M. J. Read, A. V. Lemmo, S. Ellis, M. J. Cima and C. R. Gardner, *Adv. Drug Delivery Rev.*, 2004, **56**, 275–300.

20 M. Pudipeddi and A. T. M. Serajuddin, *J. Pharm. Sci.*, 2005, **94**, 929–939.

21 D. Singhal and W. Curatolo, *Adv. Drug Delivery Rev.*, 2004, **56**, 335–347.

22 J. V. Walther and H. C. Helgeson, *Am. J. Sci.*, 1977, **277**, 1315–1351.

23 H. D. Williams, N. L. Trevaskis, S. A. Charman, R. M. Shanker, W. N. Charman, C. W. Pouton and C. J. H. Porter, *Pharmacol. Rev.*, 2013, **65**, 315–499.
24 S. Piano, A. Romano, M. Di Pascoli and P. Angeli, *Liver Int.*, 2017, **37**, 116–122.
25 J. J. McKinnon, D. Jayatilaka and M. A. Spackman, *Chem. Commun.*, 2007, 3814–3816, DOI: 10.1039/b704980c.
26 J. J. McKinnon, M. A. Spackman and A. S. Mitchell, *Acta Crystallogr., Sect. B: Struct. Sci., Cryst. Eng. Mater.*, 2004, **60**, 627–668.
27 M. A. Spackman and D. Jayatilaka, *CrystEngComm*, 2009, **11**, 19–32.
28 M. A. Spackman and J. J. McKinnon, *CrystEngComm*, 2002, **4**, 378–392.